Progress In Electromagnetics Research M, Vol. 86, 79–91, 2019

Study of the Frequency Characteristic for a Magnetically Coupled Resonant Wireless Power Transmission System with Changes of the Capacitance

Zhongqi Li[1], Yang Yuan[1], Shoudao Huang[2], Yonghong Long[1], Kaiyuan Lu[3], and Jiliang Yi[1, *]

Abstract—The resonant frequency of a magnetically coupled resonant wireless power transmission system is a core parameter that determines the performance of the system. However, how to obtain the variation law of the resonant frequency and the efficiency or output power of the system is still a difficult problem when the capacitance of each coil is changed. In this paper, a two-coil wireless power transmission system is taken as an object, and the expressions of the input impedance, frequency, efficiency, and output power are deduced. Based on these expressions, the relationships among frequency, efficiency, and output power are studied. It is concluded that there may be multiple resonant frequencies in s WPT system with the changes of capacitance. The system always features a maximum efficiency point and a maximum output power point. The frequencies of the two points are almost the same. These theories provide a feasible scheme for simultaneously achieving both a high efficiency and output power. Finally, a magnetically coupled resonant wireless power transmission system is designed and developed. Simulated and experimental results demonstrate the validity and correctness of the proposed method.

1. INTRODUCTION

In recent years, traditional wired power supply systems have been unable to satisfy requirements for mobility and special occasions because mobile devices develop rapidly, and there are some outstanding problems in traditional wired power supply systems. Therefore, wireless power transmission (WPT) technology has become a research hotspot [1–5]. This technology has broad application prospects in electric vehicles, consumer electronics, and aerospace due to its reliability.

WPT technology is mainly divided into four categories [6]: electromagnetic induction, microwave, laser, and magnetically coupled resonance according to the mechanism and mode of the power transmission. The WPT technology has a short transmission distance (in the range of cm) [7] based on electromagnetic induction. WPT technology is mainly used in long transmission distances based on microwave and laser methods. However, the strong energy of microwaves and lasers can cause fatal damage to creatures [8]. The characteristics of the magnetically coupled resonant WPT technology are as follows: (1) mid-range transmission distance (in the range of m); (2) large transmission power; (3) high transmission efficiency; (4) power supply security. A new direction has been found for the study of WPT technology [9].

The resonant frequency is a core parameter that determines the performance of a magnetically coupled resonant WPT system [10]. High efficiency and output power can be obtained when the

Received 22 July 2019, Accepted 24 September 2019, Scheduled 30 October 2019

* Corresponding author: Jiliang Yi (ieee_china@126.com).

[1] College of Traffic Engineering, Hunan University of Technology, Zhuzhou 412007, China. [2] College of Electrical and Information Engineering, Hunan University, Changsha 410082, China. [3] Department of Energy Technology, Aalborg University, Aalborg DK-9220, Denmark.

system is operated in a resonant state. At present, scholars basically consider that WPT system works in an ideal resonant state with studying the magnetically coupled WPT system. However, the following reasons may cause the system frequency drift in practical applications. (1) The inductances or capacitances are changed when the external environment changes, which result in frequency drift [11]. (2) The inductance or capacitance of the resonant coil will be changed due to some materials (such as aluminum foil, metal materials, and people, which cause the resonant frequency drift). (3) There is an error between the value of nominal resonant capacitance and the value of actual capacitance, which results in a frequency drift. (4) The temperature change of the WPT system also causes the change of the resonant capacitance, which leads to resonant frequency detuning. The transmission efficiency and output power of the system will be changed drastically, which may harm the reliability and safety of the system when the system is detuned. The common tuning methods are as follows in order to maintain the resonant state of the WPT system. (1) The resonant capacitances are adjusted by manual operation. Capacitances are tested with the help of an impedance analyzer, and then the appropriate resonant capacitances are found by experimenting one by one. However, it is difficult to achieve resonant state by manually adjusting the external resonant capacitance when there are multiple resonant coils in the WPT system [12]. (2) The external resonant capacitances are adjusted by automatic operation. The system mismatch problem can be successfully solved by using this method. However, the system device is more complicated because it requires a large number of switches to adjust the capacitances [13]. (3) The resonant frequency is found through automatic frequency tracking method. There are two main methods for frequency tracking. First, the frequency is automatically changed to maintain the system in resonance state. Secondly, the automatic frequency tracking is achieved by self-resonant technology. The advantage of the above methods is that the resonant frequency can be automatically found without an accurate resonant capacitance. However, the above methods can only randomly track a resonant frequency point, and it cannot guarantee that the resonant frequency point of the highest efficiency or maximum output power can be tracked every time when there are multiple resonant frequencies in the WPT system. Therefore, the frequency characteristic of a magnetically coupled resonant WPT system is studied in order to obtain the optimal resonant frequency.

This paper takes a two-coil WPT system as the research object. First, the expressions of efficiency and power are deduced. The relationship between the frequency and efficiency or output power is studied in depth based on these expressions. Secondly, it is concluded that there are multiple resonant frequencies in the WPT system when the resonant capacitances of the transmission coil and receiving coil are changed. The WPT system always features a maximum efficiency point and a maximum output power point. These frequencies are almost the same. Finally, a magnetically coupled resonant WPT system setup is designed and developed. Simulated and experimental results verify the validity of the theory.

2. MATHEMATICAL MODEL UNDER FREQUENCY DRIFT

Figure 1 shows schematic of the WPT system via magnetically coupled resonance. It consists of a source power, a transmission coil (Tx), a receiving coil (Rx), and a load. Parameter D is the transmission distance between the transmission coil (Tx) and receiving coil (Rx). Parameter C_{Tx} is the resonant capacitance of the transmission coil. Parameter C_{Rx} is the resonant capacitance of the receiving coil.

The two-coil WPT system can be represented in terms of lumped circuit elements (L, C, and R), as shown in Figure 2. Variable V_{s} is the AC source power, R_1 the internal resistance of Tx, R_2 the internal

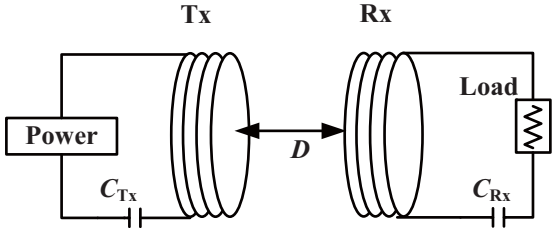

Figure 1. Schematic of the WPT system.

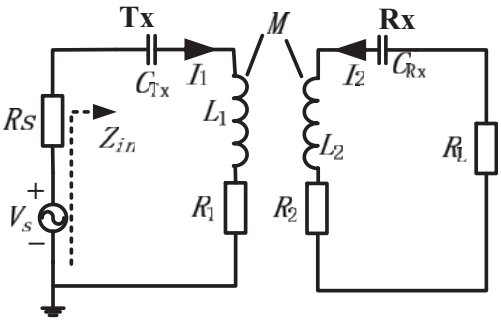

Figure 2. Equivalent circuit of the WPT system.

resistance of Rx, R_{s} the internal resistor of the power source, R_{L} the load resistor, L_1 the self-inductance of Tx, L_2 the self-inductance of Rx, M the mutual inductance between Tx and Rx, and Z_{in} the input impedance. ω_1 is the resonant angular frequency of Tx, ω_2 the resonant angular frequency of Rx, ω_0 the original resonant angular frequency, and ω the operating angular frequency. All angular frequencies are shown in Table 1.

Table 1. Angular frequencies.

Symbol	Quantity	Definition
ω	The operating angular frequency	$2\pi f$ $(0.6f_0 < f < 1.4f_0)$
ω_0	The original resonant angular frequency	$2\pi f_0$ $(f_0 = 85\,\mathrm{kHz})$
ω_1	The resonant angular frequency of the transmission coil	$\omega_1 = (L_1 C_{\mathrm{Tx}})^{-1/2}$
ω_2	The resonant angular frequency of the receiving coil	$\omega_2 = (L_2 C_{\mathrm{Rx}})^{-1/2}$

By applying Kirchhoff's voltage law (KVL), the two-coil WPT system is presented as follows [14]:

$$Z_1 \dot{I}_1 + j\omega M \dot{I}_2 = \dot{V}_{\mathrm{s}} \tag{1}$$

$$j\omega M \dot{I}_1 + Z_2 \dot{I}_2 = 0 \tag{2}$$

$$Z_1 = R_{\mathrm{s}} + R_1 + j\omega L_1 + 1/(j\omega C_{\mathrm{Tx}}) \tag{3}$$

$$Z_2 = R_{\mathrm{L}} + R_2 + j\omega L_2 + 1/(j\omega C_{\mathrm{Rx}}) \tag{4}$$

where I_1 is the current of Tx, and I_2 is the current of Rx.

The expressions of I_1 and I_2 can be obtained by solving Eqs. (1) and (2).

$$\dot{I}_1 = \frac{\dot{V}_{\mathrm{s}} Z_2}{Z_1 Z_2 + (\omega M)^2} \tag{5}$$

$$\dot{I}_2 = -\frac{j\omega M \dot{V}_{\mathrm{s}}}{Z_1 Z_2 + (\omega M)^2} \tag{6}$$

According to Eqs. (5) and (6), the expression of the efficiency is as follows:

$$\eta = \left| \frac{\dot{I}_2^2 R_{\mathrm{L}}}{\dot{V}_{\mathrm{s}} \dot{I}_1} \right| = \left| \frac{(\omega M)^2 R_{\mathrm{L}}}{Z_1 {Z_2}^2 + (\omega M)^2 Z_2} \right| \tag{7}$$

According to Eqs. (3), (4), and (7), the expression of the efficiency can be obtained as follows:

$$\eta = \left| \frac{I_2^2 R_{\mathrm{L}}}{V_{\mathrm{s}} I_1} \right| = \left| \frac{U^2 U_{\mathrm{L}}}{[(1 + U_{\mathrm{s}} + j\varepsilon_1 Q_1)(1 + U_{\mathrm{L}} + j\varepsilon_2 Q_2)^2 + (1 + U_{\mathrm{L}} + j\varepsilon_2 Q_2)U^2]} \right| \tag{8}$$

According to Eq. (6), the expression of the output power can be obtained as follows:

$$P_{\text{out}} = \left| \dot{I}_2^2 R_{\text{L}} \right| = \left| \frac{{V_{\text{s}}}^2 U^2 U_{\text{L}}}{\left[(1 + U_{\text{s}} + j\varepsilon_1 Q_1)(1 + U_{\text{L}} + j\varepsilon_2 Q_2) + U^2 \right]^2} \right| \tag{9}$$

where the source matching factor is defined as $U_{\text{s}} = \text{R}_{\text{s}}/\text{R}_1$. The load matching factor is defined as $U_{\text{L}} = \text{R}_{\text{L}}/\text{R}_2$; the coupling factor is defined as $U = \omega M/(R_1 R_2)^{1/2}$; the unload quality factor of the transmission coil is defined as $Q_1 = \omega L_1/R_1$; the unload quality factor of the receiving coil is defined as $Q_2 = \omega L_2/R_2$; the angular frequency deviation factor of Tx is defined as $\varepsilon_1 = 1 - \omega_1^2/\omega^2$; the angular frequency deviation factor of Rx is defined as $\varepsilon_2 = 1 - \omega_2^2/\omega^2$.

By differentiating P_{out} with respect to ω and equating the differential function to zero,

$$\frac{\partial P_{\text{out}}}{\partial \omega} = 0 \tag{10}$$

The analytical expression of Eq. (10) is not given because the result of Eq. (10) is too complicated. However, according to Eq. (10), it is convenient to calculate the angular frequency corresponding to the maximum output power point with the help of MATLAB.

The expression of the input impedance is defined as follows [15]:

$$Z_{\text{in}} = V_{\text{s}}/I_1 - R_{\text{s}} \tag{11}$$

According to Eqs. (3), (4), and (11), the expression of the input impedance can be obtained as follows:

$$Z_{\text{in}} = R_1 \frac{[(U^2 + (1+U_{\text{s}})(1+U_{\text{L}}) - Q_1 Q_2 \varepsilon_1 \varepsilon_2) + j(Q_1 \varepsilon_1 (1+U_{\text{L}}) + Q_2 \varepsilon_2 (1+U_{\text{s}}))][(1+U_{\text{L}}) - jQ_2 \varepsilon_2]}{(1+U_{\text{L}})^2 + Q_2^2 \varepsilon_2^2} - R_{\text{s}} \tag{12}$$

By simplifying Eq. (12), Eq. (13) can be obtained as follows:

$$Z_{\text{in}} = R_1 \frac{\left[(1+U_{\text{L}})^2 + U^2(1+U_{\text{L}}) + Q_2^2 \varepsilon_2^2 \right] + j\left[(1+U_{\text{L}})^2 Q_1 \varepsilon_1 + Q_1 \varepsilon_1 Q_2^2 \varepsilon_2^2 - U^2 Q_2^2 \varepsilon_2^2 \right]}{(1+U_{\text{L}})^2 + Q_2^2 \varepsilon_2^2} \tag{13}$$

According to Eq. (13), the input impedance angle (θ) between V_{s} and I_1 can be obtained as follows:

$$\theta = \arctan[\text{Im}(Z_{\text{in}})/\text{Re}(Z_{\text{in}})] \tag{14}$$

$$\theta = \arctan\left[\frac{(1+U_{\text{L}})^2 Q_1 \varepsilon_1 + Q_1 Q_2^2 \varepsilon_1 \varepsilon_2^2 - U^2 Q_2 \varepsilon_2}{(1+U_{\text{L}})^2 + U^2(1+U_{\text{L}}) + Q_2^2 \varepsilon_2^2} \right] \tag{15}$$

where $\text{Re}(Z_{\text{in}})$ represents the real part of the input impedance; $\text{Im}(Z_{\text{in}})$ represents the imaginary part of the input impedance; θ is the input impedance angle between V_{s} and I_1. Let Eq. (15) equal to zero ($\theta = 0$), and Eq. (16) can be obtained as follows:

$$\begin{aligned} &\left(L_1 L_2^2 - L_2 M^2\right) \omega^6 + \left[(R_2 + R_L)^2 L_1 - 2L_1 L_2^2 \omega_2^2 - L_1 L_2^2 \omega_1^2 + L_2 M^2 \omega_2^2 \right] \omega^4 \\ &+ \left[L_1 L_2^2 \omega_2^4 + 2L_1 L_2^2 \omega_1^2 \omega_2^2 - (R_2 + R_L)^2 L_1 \omega_1^2 \right] \omega^2 - L_1 L_2^2 \omega_1^2 \omega_2^4 = 0 \end{aligned} \tag{16}$$

According to Eq. (16), the new resonant frequency of the system can be obtained when the system parameters are changed. The analytic expression of each resonant frequency is not given in this paper because Eq. (16) is too complicated. It can be seen from Eq. (16) that the resonant frequency of the WPT system is mainly related to ω_1 and ω_2. For given coil parameters, the self-inductance is generally unchanged. Therefore, ω_1 is mainly affected by resonant capacitance C_{Tx}; ω_2 is mainly affected by the resonant capacitance C_{Rx}.

3. THEORETICAL CALCULATION AND SIMULATION VERIFICATION

In this section, the variation law of the new resonant frequency is studied according to Eq. (16), and the effect of the new resonant frequency on the efficiency and output power is also studied according to Eqs. (7) to (10). These studies provide a theoretical basis for the optimal efficiency or output power.

3.1. Theoretical Calculation

The frequency corresponding to the maximum efficiency and the frequency corresponding to the maximum output power are calculated when C_{Tx} or C_{Rx} is changed. The parameters of the system are shown in Table 4 in the experimental verification section. The reference resonant capacitance of the transmission coil is 9.86 nF, and the reference resonant capacitance of the receiving coil is 16.09 nF. Frequency characteristics are studied when C_{Tx} or C_{Rx} is increased based on the reference capacitance because C_{Tx} or C_{Rx} is easy to be increased by paralleling. Similarly, frequency characteristics can also be studied according to the proposed method in this paper when C_{Tx} or C_{Rx} is reduced based on the reference capacitance.

Table 2. Frequencies at the maximum efficiency point with different resonant capacitances.

C_{Rx}/nF	C_{Tx}/nF		
	16.09	17.09	18.09
9.86	78.021 kHz	93.990 kHz	93.261 kHz
	85.335 kHz		
	94.864 kHz		
10.86	75.252 kHz	74.833 kHz	75.282 kHz
	84.731 kHz	80.990 kHz	76.734 kHz
	91.602 kHz	90.741 kHz	89.946 kHz
11.86	72.841 kHz	72.332 kHz	71.927 kHz
		83.054 kHz	79.445 kHz
		87.601 kHz	87.015 kHz

Table 3. Frequencies at the maximum output power point with different resonant capacitances.

C_{Rx}/nF	C_{Tx}/nF		
	16.09	17.09	18.09
9.86	76.821 kHz	75.705 kHz	74.531 kHz
	95.652 kHz	94.510 kHz	93.612 kHz
10.86	74.746 kHz	73.872 kHz	75.282 kHz
	93.231 kHz	91.790 kHz	72.944 kHz
11.86	72.612 kHz	71.922 kHz	71.203 kHz
	91.531 kHz	89.821 kHz	88.421 kHz

According to Eq. (16), the resonant frequency corresponding to the maximum efficiency point with different resonant capacitances can be calculated with the help of MATLAB. Table 2 shows frequencies at the maximum efficiency point with different capacitances. In most cases, there are three resonant frequencies in the WPT system. Similarly, the frequencies corresponding to the maximum output power with different resonant capacitances can be calculated according to Eq. (10). Table 3 shows frequencies at the maximum output power point with different capacitances. From Table 3, there are two peaks in the output power. It is well known that the system has the lowest impedance and highest efficiency when the system is operating in a resonant state [16]. There is always a frequency corresponding to the maximum output power which is very close to the frequency corresponding to the maximum efficiency by comparing the frequencies in Table 2 and Table 3.

The efficiency is maximum at the frequency of 94.864 kHz when $C_{\mathrm{Tx}} = 9.86$ nF and $C_{\mathrm{Rx}} = 16.09$ nF according to Table 2. There is a maximum output power point in the system, and the frequency corresponding to the maximum output power point is 95.652 kHz according to Table 3. The difference

between the frequency corresponding to the maximum efficiency and the frequency corresponding to the maximum output power is only 1%, which provides a theoretical basis for simultaneously satisfying optimal efficiency and high output power.

3.2. Simulation Verification

This section verifies the correctness of the theoretical calculations in the previous section. The "Mutual inductance" model in MATLAB is used to verify the correctness of theoretical calculations. The simulation results are shown in Figure 3 to Figure 5. The WPT system exhibits pure resistance only when the input impedance angle is equal to zero, and the corresponding frequency is defined as the resonant frequency. The WPT system exhibits capacitance or inductance when the input impedance angle is not equal to zero. The efficiency of the system is reduced because some of the power will be stored in equivalent capacitance or equivalent inductance.

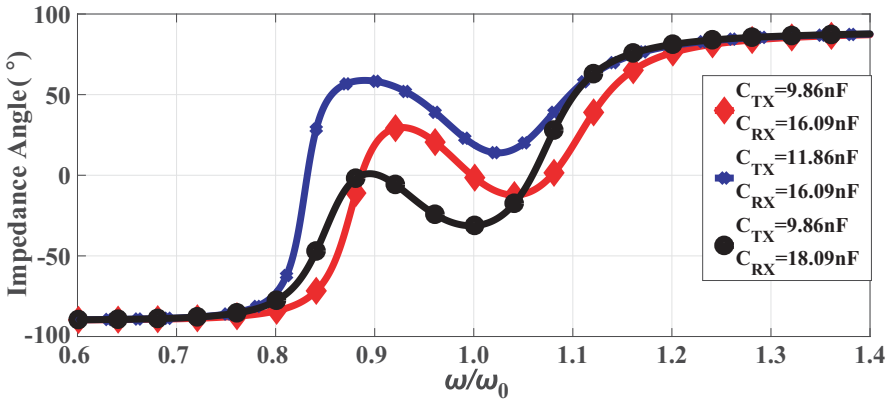

Figure 3. Relationship between impedance angle and ω/ω_0 with different capacitances.

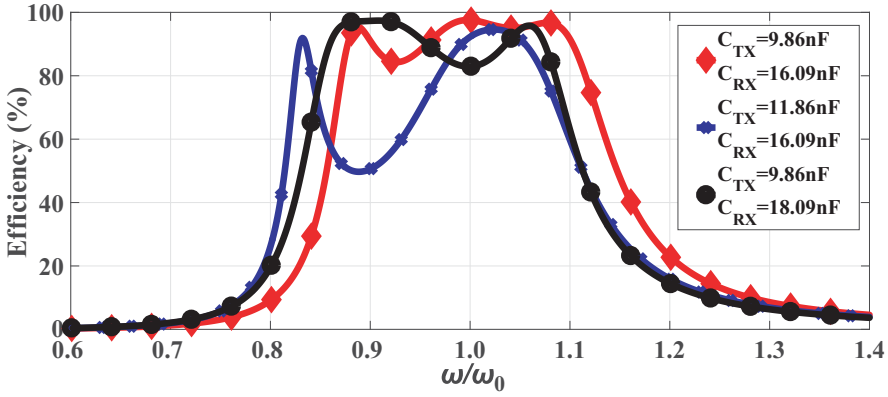

Figure 4. Relationship between the efficiency and ω/ω_0 with different capacitances.

Figure 3 shows the relationship between the impedance angle and ω/ω_0 with different capacitances. As shown in the previous section, the resonant capacitance reference of Tx is 9.86 nF, and the resonant capacitance reference of Rx is 16.09 nF. There are three resonant frequencies of 78.325 kHz, 85.378 kHz, and 94.994 kHz in the WPT system when the resonant capacitances of the transmission coil and receiving coil are both reference capacitances. There is only a resonant frequency of 72.797 kHz when the resonant capacitance of the transmission coil is increased by 2 nF based on the reference capacitance, and the resonant capacitance of the receiving coil is the reference capacitance. There is still only a resonant frequency point of 93.378 kHz when the resonant capacitance of the transmission coil is the reference

capacitance, and the resonant capacitance of the receiving coil is increased by 2 nF based on the reference capacitance.

Figure 4 shows the relationship between the efficiency and ω/ω_0 with different capacitances. The efficiencies of three resonant frequencies are 96.79%, 97.57%, and 95.98%, respectively, when the resonant capacitances of the transmission coil and receiving coil are both reference capacitances. The efficiency of the resonant frequency is 93.81% when the resonant capacitance of the transmission coil is increased by 2 nF based on the reference capacitance, and the resonant capacitance of the receiving coil is the reference capacitance. The efficiency of the resonant frequency point is 94.82% when the resonant capacitance of the transmission coil is the reference capacitance, and the resonant capacitance of the receiving coil is increased by 2 nF based on the reference capacitance.

Figure 5 shows the relationship between the output power and ω/ω_0 with different capacitances. The frequencies of two output power peaks are 76.961 kHz and 95.755 kHz, respectively, when the resonant capacitances of the transmission coil and receiving coil are both reference capacitances. The output powers at these two frequencies are 84.68 W and 113.5 W, respectively. There are also two output power peaks when the resonant capacitance of the transmission coil is increased by 2 nF based on the reference capacitance, and the resonant capacitance of the receiving coil is the reference capacitance. The frequencies of the two peaks are 72.505 kHz and 91.46 kHz. The output powers at these two frequencies are 210.7 W and 62.39 W, respectively. There are also two output power peaks when the resonant capacitance of the transmission coil is the reference capacitance, and the resonant capacitance of the receiving coil is increased by 2 nF based on the reference capacitance. The frequencies of the two peaks are 74.545 kHz and 93.67 kHz. The output powers at these two frequency points are 46.84 W and 162.9 W, respectively.

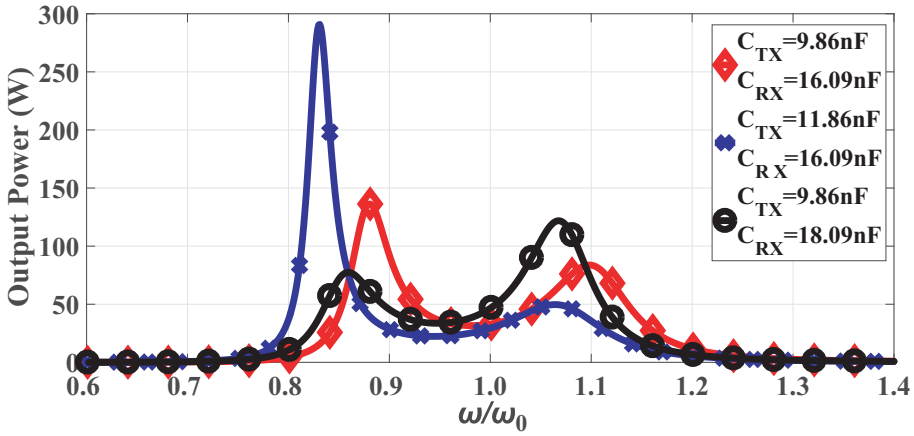

Figure 5. Relationship between the output power and ω/ω_0 with different capacitances.

From the above figures, three resonant frequencies are 78.325 kHz, 85.378 kHz, and 94.994 kHz, respectively. The efficiencies of the three resonant frequencies are 96.79%, 97.57%, and 95.98% when the resonant capacitances of the transmission coil and receiving coil are both reference capacitances. The frequencies corresponding to two output power peaks are 76.961 kHz and 95.755 kHz, respectively. It can be concluded that the differences between the frequencies of the output power peaks and the frequencies of the maximum efficiency are 1.7% and 0.8%, respectively. Similarly, the differences between the frequencies of the output power peaks and the frequencies of the maximum efficiency are 0.4% and 0.3%, respectively in the other two situations.

The simulation results are basically consistent with the calculation ones which verify the correctness of the theory. At the same time, some conclusions obtained are as follows. First, the frequency of the maximum efficiency point and the frequency of the maximum output power point are changed when the resonant capacitance shifts. Secondly, the frequency of the maximum efficiency point and the frequency of the maximum power point are not completely the same, but two frequencies are very close. Finally, the efficiency and output power of the system are increased by adjusting the operating frequency.

4. EXPERIMENTAL VERIFICATION

4.1. Experimental Setup

In order to verify the correctness of the theory, a set of experimental devices is designed and developed, including the DC voltage source, H-inverter power supply, transmission coil, receiving coil, full-bridge rectifier, and load. The experimental device is shown in Figure 6. The diagram of the experimental circuit is shown in Figure 7. The voltage regulation of the DC voltage source is ranged from 0 V to 400 V. The H-inverter is a full-bridge inverter topology, which consists of four SiC MOSFETs, and the model of the SiC MOSFET is C2M0080120D. The transmission coil is on the bottom of the wood shelf. The receiving coil is on the top of the wood shelf. The inner and outer diameters of the transmission coil are 50 cm and 60 cm, respectively, and the number of turns of Tx is 17. The inner and outer diameters of the receiving coil are 50 cm and 57 cm, respectively, and the number of turns of Rx is 13. The transmission coil and receiving coil are composed of copper wire with a diameter of 2.3 mm. The full-bridge rectifier consists of four diodes, and the model of the diode is D92. The load resistor is a gold resistor with a resistance of 15 Ω and the parasitic inductance of 9 μH. The original resonant frequency of each coil is set to 85 kHz. According to [17–19], parameters of each coil can be calculated. The resonant frequency of each coil, the self-inductance of each coil (L_i), the internal resistance of each coil (R_i), and the resonant capacitance of each coil (C_i) can be measured by an impedance analyzer. The measured parameters of each coil are shown in Table 4. The self-inductance of the transmission coil is 353.68 μH; the self-inductance of the receiving coil is 216.02 μH; and $\omega = 1/(LC)^{1/2} = 2\pi f$, where f is

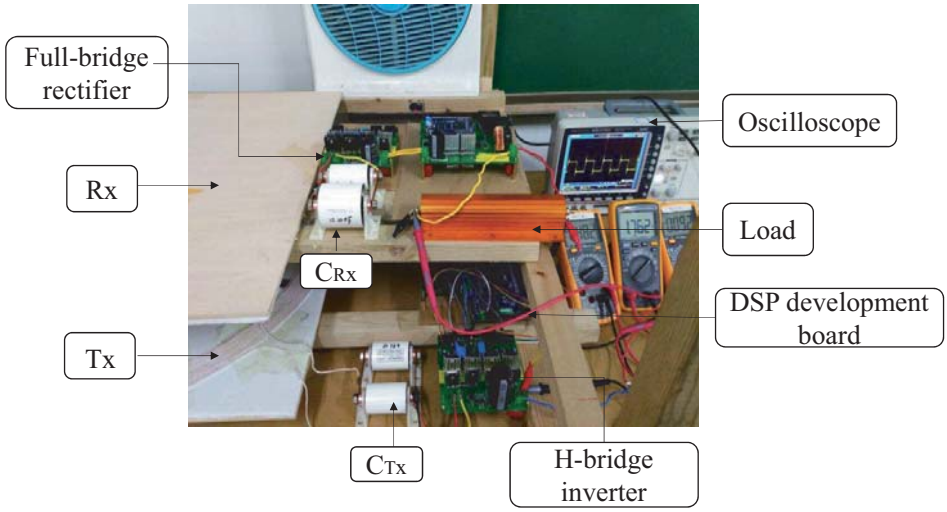

Figure 6. Physical setup of the WPT system.

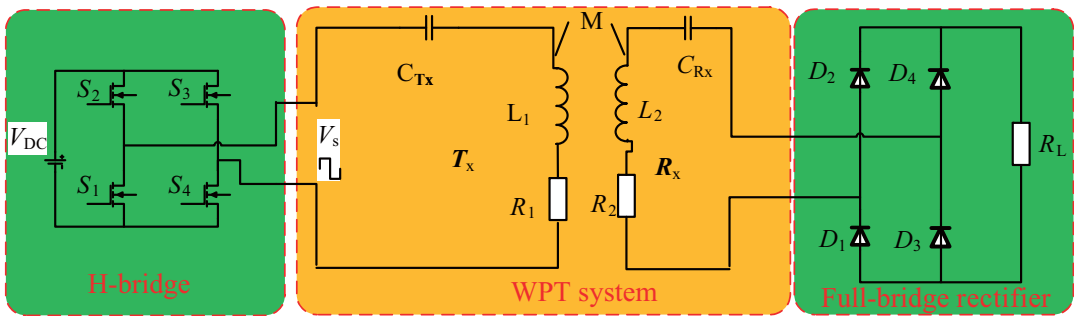

Figure 7. Diagram of the experimental circuit.

Table 4. Measured parameters of each coil.

Parameter	Physical meaning	Value
$L_1/\mu H$	The self-inductance of Tx	353.68
$L_2/\mu H$	The self-inductance of Rx	216.02
C_{Tx}/nF	The resonant capacitance of Tx	9.86
C_{Rx}/nF	The resonant capacitance of Rx	16.09
R_1/Ω	The internal resistance of Tx	0.438
R_2/Ω	The internal resistance of Rx	0.281

the operating frequency, and its value is set to 85 kHz. The resonant capacitances of the transmission coil and receiving coil are 9.91 nF and 16.20 nF, respectively. The error is 0.6% between the measured resonant capacitances and the calculated resonant capacitances due to the nominal error of the resonant capacitances. However, this error is small and can be ignored.

4.2. System Resonant Frequency Test

An impedance analyzer is used to sweep frequency of the WPT system. The results are shown in Figure 8. The blue line denotes the input impedance amplitude. The red line denotes the impedance angle. The three small red dots from the left to the right denote three resonant frequencies, which are 77.8 kHz, 83.6 kHz, and 95.9 kHz, respectively. This paper only focuses on the impedance angle. The data of the impedance angle saved by the impedance analyzer can be plotted through Excel.

Figure 9 shows the relationship between the impedance angle and frequency with different resonant

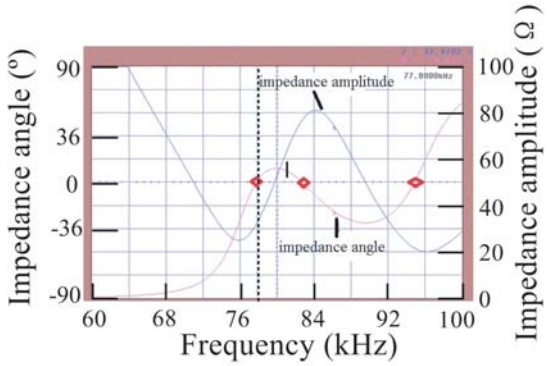

Figure 8. Relationship between impedance, characteristic angle and frequency.

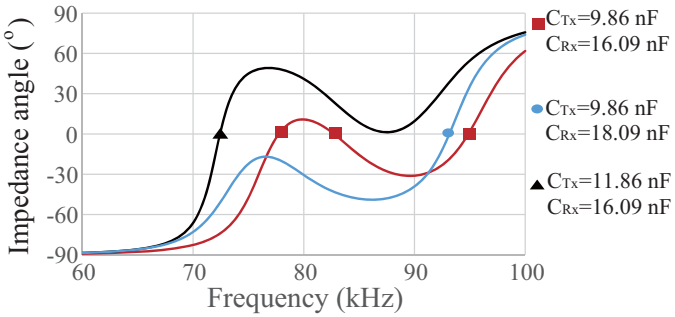

Figure 9. Relationship between impedance angle and frequency with different resonant capacitances.

capacitances. It can be seen from Figure 9 that resonant frequencies are 77.8 kHz, 83.6 kHz, and 95.9 kHz with $C_{\mathrm{Tx}} = 9.86\,\mathrm{nF}$ and $C_{\mathrm{Rx}} = 16.09\,\mathrm{nF}$; the resonant frequency is 93.2 kHz with $C_{\mathrm{Tx}} = 9.86\,\mathrm{nF}$ and $C_{\mathrm{Rx}} = 18.09\,\mathrm{nF}$; and the resonant frequency is 72.4 kHz with $C_{\mathrm{Tx}} = 11.86\,\mathrm{nF}$ and $C_{\mathrm{Rx}} = 16.09\,\mathrm{nF}$.

Resonant frequencies with different resonant capacitances are measured by the impedance analyzer. Measured results are shown in Table 5. It can be found that the errors between the measured and simulated results are less than 1.5%. The measured results are basically consistent with simulated ones, which verifies the correctness of the resonant frequency calculation method when C_{Tx} or C_{Rx} is changed.

Table 5. Measured resonant frequencies with different resonant capacitances.

C_{Rx}/nF	C_{Tx}/nF		
	16.09	17.09	18.09
9.86	77.8 kHz	94.0 kHz	93.2 kHz
	83.6 kHz		
	95.9 kHz		
10.86	74.8 kHz	74.3 kHz	74.2 kHz
	84.6 kHz	81.0 kHz	77.2 kHz
	91.6 kHz	90.6 kHz	89.8 kHz
11.86	72.4 kHz	72.0 kHz	71.4 kHz
		82.8 kHz	79.2 kHz
		87.6 kHz	86.8 kHz

4.3. Frequency, Transmission Efficiency, and Output Power Characteristics Test

The DC input voltage, DC input current, and output voltage of the load at different operating frequencies are recorded by adjusting the switching frequency of the H-inverter when the resonant capacitances of Tx and Rx are reference capacitances. The input DC voltage is set to 50 V, and the load is set to 15 Ω. Then the data are plotted as Figure 10 and Figure 11.

Figure 10 shows the relationship between the efficiency and operating frequency. The efficiency curve is not very smooth because the multimeter is not very accurate. However, the validity of theory and simulation is not affected by the error of the measured results. As shown in Figure 10, the efficiencies of 77.8 kHz, 86.2 kHz, and 95.9 kHz are 86.53%, 85.63%, and 88.12%, respectively. The efficiency of the original resonant frequency of 85 kHz is 83.7%. It can be seen that the efficiency of the new resonant

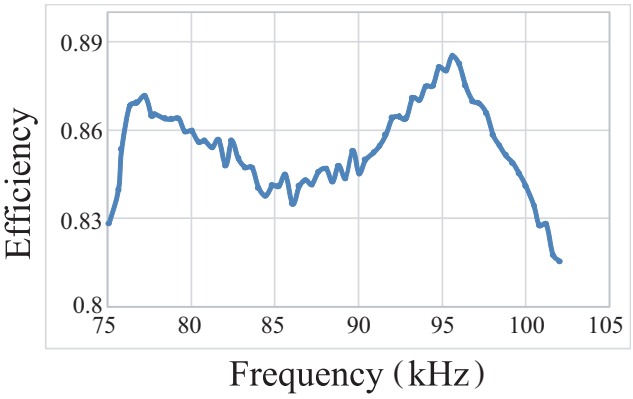

Figure 10. Relationship between the efficiency and operating frequency.

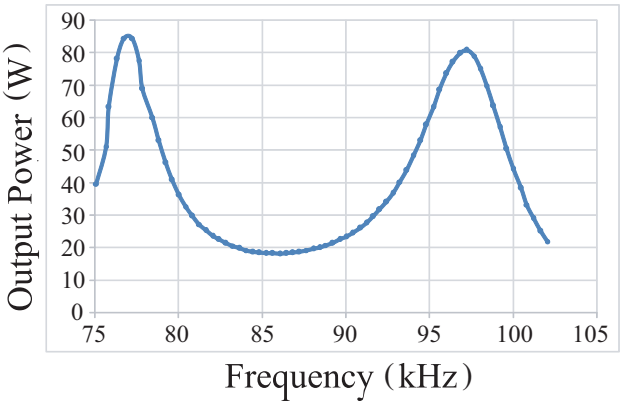

Figure 11. Relationship between the output power and operating frequency.

frequency is higher than the efficiency of the original resonant frequency.

Figure 11 shows the relationship between the output power and operating frequency. The frequencies of two output power peaks are 77.2 kHz and 97.2 kHz, respectively, according to Figure 11. The output powers of these frequencies are 84.32 W and 80.66 W, respectively. The output power is 68.92 W at the resonant frequency of 77.8 kHz. The output power is 21.42 W at the resonant frequency of 86.2 kHz. The output power is 57.72 W at the resonant frequency of 95.9 kHz. In addition, the output power is only 19.24 W at the original resonant frequency. It can be seen that the output power of the new resonant frequency is larger than the output power of the original resonant frequency.

To verify the correctness of these three resonance frequencies, the input voltage and input current of the transmission coil are tested as shown in Figures 12, 13, and 14. From these figures, the input

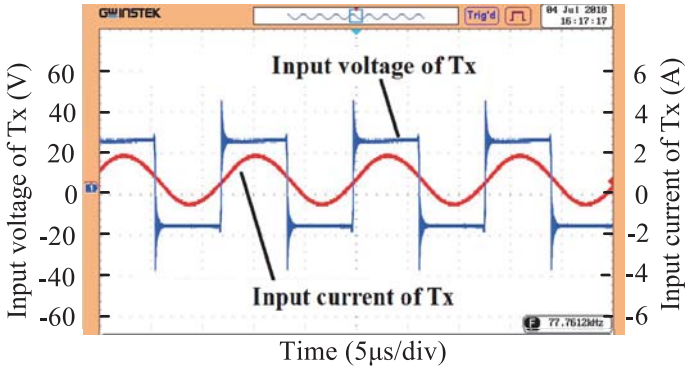

Figure 12. Voltage and current waveform at resonant frequency of 77.8 kHz.

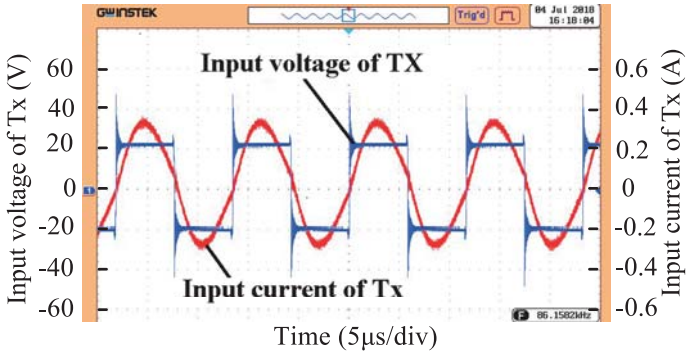

Figure 13. Voltage and current waveform at resonant frequency of 86.2 kHz.

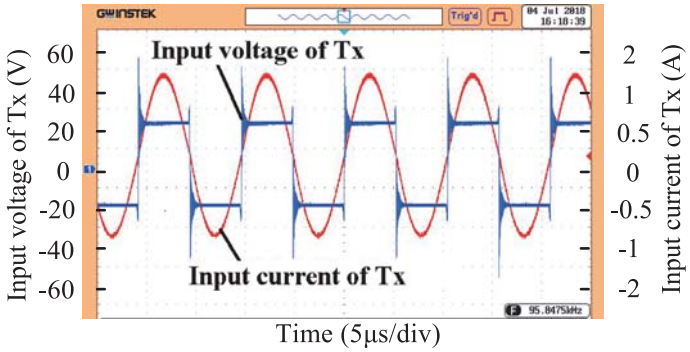

Figure 14. Voltage and current waveform at resonant frequency of 95.9 kHz.

voltage and input current are in phase at the three resonant frequencies of 77.8 kHz, 86.2 kHz, and 95.9 kHz. There is a slight error between measured resonant frequencies and calculated resonant frequencies because the addition of the full-rectifier bridge in the experimental section has an effect on the resonant frequency of the WPT system.

5. CONCLUSION

In this paper, key expressions of solving the resonant frequency and the frequency corresponding to the maximum power are deduced when the resonant capacitance of each coil is changed. Based on these key expressions, the resonant frequencies and the frequencies corresponding to the maximum output power are calculated. The frequency corresponding to the maximum efficiency is nearly the same as the frequency corresponding to the maximum output power. This provides a theory for achieving both high efficiency and output power at the same time.

Compared to the efficiency and the output power with the original resonant frequency, the efficiency is higher, and the output power is also higher with the new resonant frequency. When the resonant capacitances of the transmission and receiving coils are reference values, the efficiency is 83.7%, and the output power is 19.24 W with the original resonant frequency, whereas the efficiency is 88.1%, and the output power is 84.32 W with the new resonant frequency. The efficiency and output power are increased by adjusting the operating frequency.

In this paper, the operating frequency of the WPT system is manually adjusted. We will study the automatic frequency tracking technology in the future to meet the practical application. There may be multiple resonant frequencies based on the theory of this paper. Therefore, how to track the optimal frequency is still a problem.

ACKNOWLEDGMENT

This work was supported in part by the National Natural Science Foundation of China under Grant 61104088, in part by the Hunan Provincial Department of Education under Grant 17C0469, in part by Hunan Provincial Natural Science Foundation of China under Grant 2018JJ3127 and 2019JJ60055, in part by Zhuzhou City Natural Science Foundation of China.

REFERENCES

1. Zhang, Y. M. and Z. M. Zhao, "Frequency decrease analysis of resonant wireless power transfer," *IEEE Trans. Power Electron.*, Vol. 29, No. 3, 1058–1063, Mar. 2014.
2. Liu, Z. and Z. Z. Chen, "A magnetic tank system for wireless power transfer," *IEEE Trans. Power Electron.*, Vol. 27, No. 5, 443–445, May 2017.
3. Ng, W. M. and S. Y. Ron Hui, "Two- and three-dimensional omnidirectional wireless power transfer," *IEEE Trans. Power Electron.*, Vol. 29, No. 9, 4470–4474, Sept. 2014.
4. Zhang, Y. M. and T. Lu, "Selective wireless power transfer to multiple loads using receivers of different resonant frequencies," *IEEE Trans. Power Electron.*, Vol. 30, No. 11, 6001–6005, Nov. 2015.
5. Chen, L. and S. Liu, "An optimizable circuit structure for high-efficiency wireless power transfer," *IEEE Trans. Circuits Syst. I Reg. Papers*, Vol. 59, No. 9, 2065–2074, sept. 2014.
6. Zhang, J. and X. Yuan, "Comparative analysis of two-coil and three-coil structures for wireless power transfer," *IEEE Trans. Power Electron.*, Vol. 30, No. 1, 341–352, Jan. 2017.
7. Lin, D. and S. Y. R. Hui, "Mathematical analysis of omnidirectional wireless power transfer — Part-I: Two-dimensional systems," *IEEE Trans. Power Electron.*, Vol. 32, No. 1, 625–633, Jan. 2017.
8. Jolani, F. and Y. Yu, "A planar magnetically coupled resonant wireless power transfer system using printed spiral coils," *IEEE Antennas Wireless Propag. Lett.*, Vol. 13, No. 2, 1648–1651, May 2014.
9. Kurs, A. and A. Karalis, "Wireless power transfer via strongly coupled magnetic resonances," *Science*, Vol. 317, No. 5834, 83–86, Mar. 2007.

10. Chabalko, M. J. and A. P. Sample, "Three-dimensional charging via multimode resonant cavity enabled wireless power transfer," *IEEE Trans. Power Electron.*, Vol. 30, No. 11, 6163–6173, Nov. 2015.
11. Li, S. and C. C. Mi, "Wireless power transfer for electric vehicle applications," *IEEE J. Emerg. Sel. Topics Power Electron.*, Vol. 3, No. 1, 4–17, Mar. 2015.
12. Hui, S. Y. R., "Past present and future trends of non-radiative wireless power transfer," *CPSS Trans. Power Electron. Appl.*, Vol. 1, No. 1, 83–91, Dec. 2016.
13. Zhong, W. X. and C. K. Lee, "Wireless power domino-resonator systems with noncoaxial axes and circular structures," *IEEE Trans. Power Electron.*, Vol. 27, No. 11, 4750–4762, Nov. 2012.
14. Chi, K. L. and W. X. Zhong, "Effects of magnetic coupling of nonadjacent resonators on wireless power domino-resonator systems," *IEEE Trans. Power Electron.*, Vol. 27, No. 4, 1905–1916, Apr. 2012.
15. Cannon, B. L. and J. F. Hoburg, "Magnetic resonant coupling as a potential means for wireless power transfer to multiple small receivers," *IEEE Trans. Power Electron.*, Vol. 24, No. 7, 1819–1825, Apr. 2012.
16. Chabalko, M. J. and J. Besnoff, "Resonantly coupled wireless power transfer for non-stationary loads with application in automotive environments," *IEEE Trans. Ind. Electron.*, Vol. 64, No. 1, 91–103, Jan. 2017.
17. Jayathurathnage, P. K. S. and A. Alphones, "Optimization of a wireless power transfer system with a repeater against load variations," *IEEE Trans. Ind. Electron.*, Vol. 64, No. 10, 7800–7809, Oct. 2017.
18. Zhang, C. and D. Lin, "A novel electric insulation string structure with high-voltage insulation and wireless power transfer capabilities," *IEEE Trans. Power Electron.*, Vol. 33, No. 1, 6163–6173, Jan. 2018.
19. Ludois, D. C. and J. K. Reed, "Capacitive power transfer for rotor field current in synchronous machines," *IEEE Trans. Power Electron.*, Vol. 27, No. 11, 4638–4645, Nov. 2012.